

# Molecular dynamic simulation suggests stronger in-silico docking of Omicron spike on ACE2 than Wild but weaker than Delta SARS-CoV-2 variants can be blocked by engineered S1-RBD fraction

Dipannita Santra

Oriental Institute of Science and Technology

Smarajit Maiti (✉ [maitism@rediffmail.com](mailto:maitism@rediffmail.com))

Oriental Institute of Science and Technology <https://orcid.org/0000-0002-1354-1303>

---

## Research Article

**Keywords:** SARS CoV-2, Wild Delta and Omicron variant, comparative affinity, preventive blocking/docking, 59 amino-acid RBD-cut

**Posted Date:** June 9th, 2022

**DOI:** <https://doi.org/10.21203/rs.3.rs-1451089/v1>

**License:** © ⓘ This work is licensed under a Creative Commons Attribution 4.0 International License.

[Read Full License](#)

---

# Abstract

**Background:** The SARS-CoV-2 claimed millions lives globally. Occurring from Wuhan (Wild-type) in December, 2019, it constantly mutated to Omicron (B.1.1.529) the predecessor to Delta.

**Objectives:** Omicron having ~32 spike-mutations has variable infectivity-multiplicity-immunoinvasive properties. Understanding of its mutational-effect on ACE2-binding/disease-severity and developing preventive/therapeutic strategies are important.

**Methods:** The binding-affinities of Wuhan/Delta/Omicron spikes (PDB/GISAID/SWISS-MODEL) were docked (HADDOCK2.4) with ACE2 and compared by competitive-docking (PRODIGY). The protein structural-stability was verified by kinetic-data/Ramachandran-plot (Zlab/UMassMedBioinfo). After several trials, a 59 amino-acid (453ARG-510VAL) peptide-cut (Expasy-server) of the Wild-spike-RBD with some desired mutants (THR500SER/THR500GLY/THR500ALA/THR500CYS) were blindly/competitively docked (PyMOL-V2.2.2) to block the Omicron-ACE2 binding. We examined Molecular-Dynamic-Simulation (*iMOD-server*, with 9000-cycles/300k-heating/1-atm pressure for system-equilibration for 50ns-run) of ACE2 and two CUTs with different SARS-CoV-2 variants.

**Result:** The binding-affinity of Omicron-ACE2 is slightly higher than the rest two in competitive-docking-setup. During individual (1:1) docking, Omicron showed little higher than Wild-type but much weaker binding-affinity than Delta. Competitive-docking suggests that ten H-bonding (1.3Å-2.4Å) with highly favorable energy-values/Van-der-Walls-force/Haddock-score for more stable-binding of Omicron-RBD with ACE2. Blind-docking of different CUTs (wild/mutants) and Omicron to ACE2 completely rejected the Omicron-RBD from ACE2-target. The best blocking/binding affinity of -16.4 and -13Kcal/mole were observed in case of THR500SER and THR500GLY, respectively with multiple H-bonding 1.9Å-2.2Å. These are supported by the MD-simulation results.

**Conclusion:** So the spike binding affinities were Delta>Omicron>wild in 1:1 docking with ACE2. Considering the Wild-type is non-existing nowadays, Omicron showed less ACE2 binding property. The 59Cut of spike-RBD and its mutants THR500SER/THR500GLY may be further screened as universal blocker of this virus.

## Introduction

The SARS-CoV-2 pandemic has been surging all over the world for two years. According to the statistical report of the World Health Organization (WHO), more than 260 million confirmed cases and over five million deaths have been reported [1]. The original (Wuhan) Severe Acute Respiratory Syndrome coronavirus 2 (SARS-CoV-2) viruses that was first identified at the end of December 2019 and was followed by a wave that peaked in July 2020 and end in September 2020. SARS-CoV-2 evolved timely and a variety of variants emerged.

WHO classified them into three types: a) variants of concern (VOCs), b) variants of interest (VOIs) and c) variants under monitoring (VUMs). The second wave which caused by the Beta (B.1.351 / 501Y.V2 / 20H) variant was peaked in January 2021 and end in February 2021. The third wave which peaked in July and end in September 2021, was driven by Delta (B.1.617.2 / 478K.V1 / 21A) variant [2]. In the late November 2021, a new variant named Omicron (B.1.1.529 / 21K) was designated as the fifth VOC by WHO. The emergence of Omicron variant was first detected in South Africa, raised concerns that based on at least 32 mutations in spike proteins. Many of which located in the receptor binding domain (RBD). In addition, Omicron has 3 deletions and 1 insertion in the spike protein [3].

The effects of most of the remaining Omicron mutations are not known, resulting in a high level of uncertainty about how the full combination of deletions and mutations will affect viral behavior and susceptibility to natural and vaccine-mediated immunity. Several reports provide preliminary indications on more transmissibility, immune escape and severity of the Omicron variant. But recent report suggests unlike previous variants its less severe nature due to failure to penetrate the lungs tissues in the healthy individuals. But the nature of the severity in the co-morbid individuals is yet to be confirmed. This is also to be established the actual impact of Omicron in a non-infected and non-vaccinated individuals. More data are needed to characterize the null or several factorial effects alone or in combination. Omicron has some deletions and more than 30 mutations, overlap with those in the alpha, beta, gamma, or Delta VOCs [4]. N501Y increases binding to the ACE2 receptor to induce higher transmissibility [5] and the combination of N501Y and Q498R may increase binding affinity even more; however, other substitutions in the Omicron spike protein are expected to decrease binding to ACE2. Omicron does not infect cells deep in the lung tissues as readily as it does those in the upper airways and after a few days, the concentration of virus in the lungs of animals infected with Omicron was at least ten times lower than that in rodents infected with other variants [6]. Other studies reveals that Omicron may be over 10 times more contagious than the original virus or about 2.8 times as infectious as the Delta variant [7].

The Omicron variant when combined with the H69/V70 deletion, the transmissibility might be further increased [8]. H655Y is proximal to the furin cleavage site and may increase spike cleavage, which could also increase transmission. P681H has been shown to enhance spike cleavage, which could help transmission. This mutation is found in Alpha and an alternate mutation at this position (P681R) is found in Delta. Previous studies have clarified that D614G is associated with higher upper respiratory tract viral loads and the younger age of patients [9–11].

So far, several drugs have been tested in COVID-19 at its mild, moderate and severe conditions. And for the preventive strategies a significant number and types of vaccines have been used globally. Several reports reveal the sharp failure of the vaccines and that is demonstrated by the epidemiological or vaccinated patient's sera neutralization data. We examined its sensitivity to 9 monoclonal antibodies (mAbs) clinically approved or in development, and to antibodies present in 115 sera from COVID-19 vaccine recipients or convalescent individuals. Omicron was totally or partially resistant to neutralization by all mAbs tested. Sera from Pfizer or AstraZeneca vaccine recipients, sampled 5 months after complete vaccination, barely inhibited Omicron. booster Pfizer dose as well as vaccination of previously infected

individuals generated an anti-Omicron neutralizing response, with titers 6 to 23 fold lower against Omicron than against Delta[12]. we noted that the activity of 17 of the 19 antibodies tested were either abolished or impaired, including ones currently authorized or approved for use in patients. In addition, we also identified four new spike mutations (S371L, N440K, G446S, and Q493R) that confer greater antibody resistance to B.1.1.529 [13]. Omicron subsequently and swiftly replaced the circulating Delta and other variants. The genome surveillance data shows the comparison between predicted and observed fractions of Omicron, Delta, and other variants. Omicron was estimated to be 4.2 times (95% confidence interval (CI): 2.1, 9.1) greater than that of the Delta variant. It was found 3.3 times more transmissible than the Delta variant. [14].

But it is evident that the hospitalization or the case fatality (CFR) is very lower in the Omicron infected cases. In earlier and also in recent periods, several Angiotensin Receptor Blockers (ARBs) exhibited some protecting effects. In addition to the antihypertensive effects, these drugs manifested some anti-inflammatory effects also. The ARBs are found to be protective in severe acute respiratory syndrome caused by the virus. Moreover, in some cases ACE-inhibitors and ARBs were also found to be associated with decreased mortality [15].

In this background, the blocking of the viral spike and the ACE2 binding was studied in the present study. A comparative in silico study was done to evaluate the ACE2 binding with Wuhan (wild), Delta and the Omicron variants of SARS CoV-2. Small peptide from the globally conserved Spike variants were designed with or without mutations and docking effects were tested with ACE2 in presence of the Omicron spike.

## Materials And Methods

### 1. Protein Structure Retrieval, prediction by analysis

The X-ray crystallography and electron microscopy structure were retrieved from of were retrieved from RCSB Protein Data Bank (<https://www.rcsb.org>) in PDB format. That PDB ID, used in this study were 4APH, 7CWN and 7KRQ representing Human angiotensin-converting enzyme 2 receptor (ACE2), human coronavirus (SARS CoV2) spike glycoprotein and another variant of concern B.1.617.2 (now delta) spike protein respectively. Recently, a new SARS-CoV-2 variant B.1.1.529 (Omicron) was detected from South Africa. The spike protein of the Omicron variant is characterized by at least 30 amino acid substitutions, three small deletions, and one small insertion. Notably, 15 of the 30 amino acid substitutions are in the receptor binding domain (RBD). There are also a number of changes and deletions in other genomic regions. H69-, V70-, G142-, V143, Y144-, N211- of which 69/70 deletions resulted in the failure of the S-gene target. Other substitutions in the spike protein are A67V, T95I, Y145D, G339D, S371L, S373P, S375F, K417N, N440K, G446S, S477N, T478K, E484A, Q493R, G496S, Q498R, N501Y, Y505H, T547K, D614G, H655Y, N679K, P681H, N764K, D796Y, N856K, Q954H, N969K, and L981F. Of these, mutations at H655Y, N679K, and P681H in the S1-S2 furin cleavage site of the Omicron variant might be associated with increased transmissibility [16]. We manually prepared Omicron spike protein from Wild type SARS-COV-2

spike protein (PDB- 7CWN). From our previous study, we prepared some short CUTs segments with 84 amino acid sequence for analyzed the blocking between different nCoV2 and ACE2 receptor binding at RBD domain [17]. Here we prepared new short CUTs segment from previous 84 CUTs with 59 amino acids in two steps; CUT segment was prepared from the tertiary structure of 7CWN and the respective CUT were subjected to SWISS-MODEL for tertiary structure prediction.

## 2. Structural modification

The selected PDB structures were found with different molecules like H<sub>2</sub>O, NAG etc. Whereas, COVID 19 spike glycoprotein showed with multiple NAG unit at different position. So, for molecular docking study different attached molecules were removed from the receptor molecules and manually prepared spike proteins with exact amino acid position mutations using Pymol molecular visualization software [18]. After removal, receptor molecules were saved as .pdb file for further analysis. After tertiary structure prediction was performed to understand if mutation could elevate the binding affinity of the cut or not. One point mutation was performed at THR500 position replacement with THR500SER named as CUT1 or T500S, THR500CYS as CUT2 or T500C; THR500GLY as CUT3 or T500G and THR500ALA as CUT4 or T500A. For molecular docking study different attached molecules were removed from the receptor molecules, manually prepared spike proteins with exact amino acid position mutations and different CUTs segments were prepared using Pymol molecular visualization software [18]. After removal, receptor molecules were saved as .pdb file for further analysis.

## 3. Ramachandran plot analysis

Ramachandran Plot server [19] was used for protein 3D structure quality structures assessment [<https://zlab.umassmed.edu/bu/rama/>]. We observe Ramachandran plot on number of residues present in highly preferred region and allowed regions, SARS-Cov2 Wild 94.5%, DELTA94.5% and Omicron 94.402% were found as a very good quality structure. We also observe Ramachandran plot of docked complexes and select best structures [Table S4].

## 4. Molecular docking studies

### *Surface-Topology Calculation of Proteins*

Protein pocket and cavity properties are characterized by the solvent accessibility factor. The second water molecule is restricted for enter after first one occupy these areas. The CASTp: Computed Atlas of Surface Topography of Protein ([http://sts.bioe.uic.edu/castp/index.html?j\\_5e8c7bec25090](http://sts.bioe.uic.edu/castp/index.html?j_5e8c7bec25090)) was used in the current study to characterize the pocket and cavity.

The Molecular Docking between Human ACE2 and different mutated spike proteins were individually and competitive blind docking through HADDOCK 2.4 web server [20] to check the highest and lowest binding affinity with ACE2 receptor. Also blind docking was performed of selected mutated CUTs with ACE2 and Omicron variant were performed HADDOCK 2.4 server. We only analyze the binding of CUTs segments with ACE2 and Omicron because our previous study already checks the binding affinity of CUTs segments

with SARS-CoV2. HADDOCK is an integrative platform for the modeling of biomolecular complexes. It supports a large variety of input data and deal with a large class of modeling problems including protein-protein, protein-nucleic acids and protein-ligand complexes, including multi-bodies assemblies. It also allows to define specific unambiguous distance restraints (e.g. from MS cross-links) and supports a variety of other experimental data including NMR residual dipolar couplings, pseudo contact shifts and cryo-EM maps. It calculates the docking transformation between two molecules to get the best molecular interface complementarities which finds out the binding affinity between biomolecule complexes. HADDOCK analyze the protein-protein docking from different angle through HADDOCK score, RMSD from the overall lowest-energy structure, Van der Waals energy, Electrostatic energy, Desolvation energy, Restraints violation energy, Buried Surface Area and Z-Score.

## **5. Docking result and Binding affinity analysis of different docked molecules**

Each sets of molecular docking were analyzed using PyMol molecular visualization software [18]. The presentation of docking structures and interactive bonds were represented through technical and transparent surface analysis mainly. To understand the binding between different docked molecules, each pairs were individually subjected to PRODIGY tool on HADDOCK server. PRODIGY was used to analyze the binding affinity of protein-protein and protein-small molecules complexes and also allows classifying crystallographic interfaces as biological or not [21]. The best structures from the docking result were accepted. Based on the previous study for complete displacement of nCoV2 spike protein from ACE2 RBD through CUTs segment, the highest binding affinity of CUTs with ACE2 RBD and Omicron variant the best CUT was selected for further analysis. Binding affinity quantifies the binding strength of ligand to a protein.

## **6. Evaluation of H-bonding in a competitive docking analysis.**

Observation of the H bonding length of amino acid residues between ACE2 receptor and original SARS-CoV-2 isolate Wuhan-Hu-1, the Delta mutant and Omicron mutant were demonstration by PyMol visualized system to recognize the H bond length between amino acid residues short or long. It was also observed that the H-bond interaction in short CUTs segments with ACE2 and Omicron spike protein.

## **7. Energetic and Kinetic data analysis**

During the generation of the HADDOCK score, cluster-size based RMSD valued and other bond energy values i.e. Van der Waals, Electrostatic Desolvation energy were evaluated. Binding affinity ( $\Delta G$  (kcal mol<sup>-1</sup>) Dissociation constant [Kd (M) at 25.0 °C] explained the strength and the affinity of the interactions.

## **8. Molecular dynamics simulation study of different VOCs of SARS-CoV 2 with human ACE2 and two CUTs sequences**

Based on the docking results, we performed molecular dynamics analysis studies on the selected lowest energy valued and best posed docking complex. The MD simulations were carried out by iMod server (iMODS) (<http://imods.chaconlab.org/>) [22] at 300K constant temperature, 1 atm constant pressure at

molecular mechanics level. The iMod server gives a convenient interface for this enhanced Normal mode analysis (NMA) methodology in inner coordinates. The web interface is very spontaneous and responsive to all major browsers and even to modern mobile appliances. Users can perform NMA or molecular dynamics simulate feasible trajectories between two conformations and interactively explore in 3D the resulting structures, trajectories, animations and even for large macromolecules. Finally, 50 ns molecular dynamics simulation was carried out for all the complexes such as different VOCs of SARS-CoV 2 with ACE2 and two CUT 59 sequences (wild 59 and T500S) with Omicron variants.

For structural stability analysis for docking and simulations, providing an RMSD (Root Mean Square Deviation) or root-mean-square deviation is a standard measure of structural distance between two proteins. To simulate feasible transitions, the initial structure is iteratively deformed along the lowest modes while the root mean square deviation (RMSD) to a target structure is minimized. Two initial superimposition methods can be selected: either global [23] or local [24]. Whereas the former considers all atoms for the RMSD, the latter favors the overlap between most similar regions.

## Results And Discussuion

Report reveals that the major clinical manifestations developed by the Omicron variant is "mild infection", including headache, body ache, muscles ache, cough, fever, generalized myalgia, and severe fatigue. Nevertheless, it is infecting younger and middle-aged groups [25]. More particular, the incidents of higher rate of infections are not associated with the severity of the infection outcome. At this time point, with the generation of new SARS CoV-2 variants like Delta followed by the Omicron need to be considered in association with some other factors like global vaccination, global pre-infection (by predecessor variants) and restrictions-lockdown. The interactive role of these factors may have some influences on the infection and disease severity by Omicron or other new variants. Report reveals that the sera collected from the Omicron infected person has a significant in vitro neutralization effect of Omicron variant with developing antibody response. Notwithstanding, there was an enhancement of several fold of Delta virus neutralization by this sera which may result in decreased ability of Deltato re-infect those individuals [26].

In the current study we are presenting by the in silico study the comparative analysis binding/docking parameters of SARS CoV-2 Wuhan, Delta and Omicron variants with human ACE2. We further analyzed the effects of the 59 amino acids of RBD fraction of the SARS CoV-2 and its several mutants THR500SER/GLY/ALA/CYS docking/blocking effects on ACE2 Omicron spike binding. Beside the individual spike variant binding with ACE2, comparative/combined binding of different spikes were also evaluated to predict which is more infective/transmissible. Our present results suggest few considerations.

### 1. SARS-COV2 and Omicron spike proteins binding with Human ACE2 receptor

The Spike glycoprotein's of both variant initially binds to the [Angiotensin Converting Enzyme 2 \(ACE2\)](#) present at the host cell surface and then the viral entry gradually proceeds. This ACE2 attachments site

remains folded until it reaches the receptor. Just before ACE2 attachment in SARS-CoV2 spike protein's flexible part become unfolded and the attachment site become exposed [27]. Individual docking of ACE2 and three different spike protein results were observed [figure 1]. According to the competitive multi docking studies between ACE2-SARSCoV2 – Omicron showed highest docking score of  $-194.5 \pm 5.1$ . The cumulative energy calculation of Van der Waals energy, desolvation energy and electrostatic energy represented the negative value of  $-98.0 \pm 9.9$ ,  $-50.9 \pm 13.4$  and  $-315.3 \pm 105.1$  respectively [ Table S1a].

Electrostatic energy represents the potential energy of a system placed within the time-invariant electric field [28] where the positive value indicated the repulsion and negative value indicated the surface attraction between two molecules [29]. Here, SARS-CoV-2 showed higher binding affinity with ACE2 with a value  $-9 \Delta G$  (kcal mol<sup>-1</sup>) and it also showed some Dissociation constant value of  $2.50E-07$ . In contrary, molecular docking with ACE2 and Omicron showed comparable binding affinity of  $-7.4 \Delta G$  (kcal mol<sup>-1</sup>) [Table S2a] at the binding site. The active site of ACE2 comprises of different amino acids, i.e. TYR83, GLN24, LYS31, GLU35, LYS353, ASP38 and LYS68 with which interaction of TYR489, AS487, TYR453, ARG403, ASP405, TYR505, GLY496 and ASN501 different amino acids of SARS-CoV2 binding sites were observed respectively [Figure 2; Table S3a].

The active site of ACE2 comprises of different amino acids, i.e. ASP67 and GLU75 with which interaction of LYS478, ASN487 and TYR489 different amino acids of Omicron variant binding sites were observed respectively [Figure 2; Table S3a]. At the surface of ACE2 and spike glycoprotein interaction, all the amino acids interact with each other with the formation of H-bonds [Table S3a].

## 2. Delta and Omicron spike proteins binding with Human ACE2 receptor

Molecular docking with Delta variant and Omicron variant with ACE2 receptor revealed that the highest docking score value of  $-137.6 \pm 12.1$ . The calculation of Van der Waals energy, desolvation energy and electrostatic energy represented the negative value of  $-80.4 \pm 4.0$ ,  $-31.8 \pm 2.9$  and  $-284.8 \pm 64.1$  respectively [table S1a]. Here, DELTAvariant showed higher binding affinity with ACE2 with a value  $-9.7 \Delta G$  (kcal mol<sup>-1</sup>) and it also showed some Dissociation constant value of  $7.70E-08$  [table S2a]. Contrarily, Omicron variant did not show any binding affinity against ACE2 in presence of the DELTA. It could be possible that the 15 mutations of RBD<sub>Omicron</sub> are not evenly distributed in RBD, but rather crowded in its RBM with 10 residues, *viz.*, N440K, G446S, S477N, T478K, E484A, Q493K, G496S, Q498R, N501Y and Y505H [30]. For that reason, Omicron variant have lower binding affinity than DELTA.

The active site of ACE2 comprises of different amino acids, i.e. GLN42, ASP38 and LYS353 with which interaction of ASP571, ARG567 and GLN563 different amino acids of Delta binding sites were observed respectively [Figure 3; Table S3a]. The H-bond length also observed between amino acid residues [Table S3a]. On the other hand, molecular docking with of ACE2 and Omicron showed no binding affinity and no binding occur [Table S2a].

## 3. Comparative study between 3 spike proteins binding with Human ACE2 receptor



According to the docking result between ACE2, Delta, Omicron and SARS-CoV-2 showed the highest docking score value of  $-250.8 \pm 19.4$ . The calculation of Van der Waals energy, desolvation energy and electrostatic energy represented the negative value of  $-157.9 \pm 11.4$ ,  $-451.1 \pm 46.0$  and  $-63.6 \pm 7.8$  respectively [table S1a]. The binding affinity of DELTA, Omicron with ACE2 was  $-7.1$  and  $-9.9$  respectively [table S2a]. But molecular docking with ACE2 and SARS-CoV2 showed no binding affinity. From the above two results, we analyze that Delta is stronger binding affinity with ACE2 than Wild type SARS-CoV-2 and Omicron. When we study MD stimulation of ACE2 binding affinity with 3 different strains together, Omicron variant showed comparable binding affinity with human ACE2 in comparison with Delta strain.

According to Bloom et al [31], it was found that 9 RBD<sub>Omicron</sub> mutations (S371L, S373P, S375F, K417N, G446S, E484A, G496S, Q498R, Y505H) should decrease the binding affinity to ACE2 while the other 6 mutations (G339D, N440K, S477N, T478K, Q493K, N501Y) should increase the binding affinity, resulting in a challenge of predicting its transmissibility and potential immune evasion risk. The binding site of ACE2 comprises of different amino acids, i.e. GLU329, TYR41, TYR83 and SER19 with which interaction of LYS558, GLN563, LYS462 and GLU471 different amino acids of Delta binding sites were observed respectively [Figure 4; Table S3a]. The binding site of ACE2 comprises of different amino acids, i.e. GLU87 and LYS112 with which interaction of ARG498 and ALA372 different amino acids of Omicron binding sites were observed respectively [Figure 4; Table S3a]. The H-bond length also observed between amino acid residues [table S3a].

#### 4. Measurement of binding affinity and kinetics of different CUTs segment

Here we investigate the blind docking of Wild 59, T500S, T500C, T500G and T500A interaction with ACE2 and Omicron showed the docking score value of  $-175.1 \pm 13.8$ ,  $-163.1 \pm 13.8$ ,  $-172.2 \pm 26.8$ ,  $-163.6 \pm 9.4$  and  $-174.0 \pm 11.9$  respectively [table S1b]. According to Binding affinity result, the binding affinity between Wild 59 segments and Omicron variant was  $-12.5 \Delta G$  (kcal mol<sup>-1</sup>), T500S and Omicron variant  $-16.4 \Delta G$  (kcal mol<sup>-1</sup>), T500C and Omicron variant  $-12.2 \Delta G$  (kcal mol<sup>-1</sup>), T500G and Omicron variant  $-13 \Delta G$  (kcal mol<sup>-1</sup>) and T500A and Omicron variant  $-12.3 \Delta G$  (kcal mol<sup>-1</sup>) [table S2b].

Among the mutated CUTs segment, we showed that the best binding affinity between CUTs and spike protein was  $-16.4 \Delta G$  (kcal mol<sup>-1</sup>) because the lower energy and higher negative value means the higher stability of the complex. Due to the sequence shorting may be T500S cut have higher binding affinity than 84 cut segments. So, we choose only T500S cut segment for further analysis and Wild 59 cut segment as a control. After analysis the H-bond pattern, T500S cut showed 6 interactions with Omicron spike protein at RBD site ranged from  $1.9 - 2.1 \text{ \AA}$  [table S3b], whereas Wild 59 cut showed 5 interactions ranged from  $1.9 - 2.8 \text{ \AA}$  [table S3b]. The binding affinity values and H-bond interactions of T500S were comparatively higher than the Wild 59-cut.

The interaction site of T500S cut comprises of different amino acids ASN137, TYR 185, VAL 187, ASN 164 and SER 154 with which interaction of ASN450, TYR501, PRO499, CYS488, GLY485 and ALA484 different amino acids of Omicron binding sites were observed respectively [Figure 6; Table S3b]. Our

previous study analyze that the CUT segments of 84 amino acids after molecular docking with ACE2 receptor and SARS-CoV-2, the docked structures were either partial or complete interactive distortions of spike glycoprotein from ACE2 receptor was observed. But when we observed the docking structure of T500S cut segment, Omicron and ACE2, T500S cut bind at RBD site of Omicron and ACE2 bind different position of Omicron not in the RBD active site. The docking structure of WILD59 segment Omicron and ACE2 was shown WILD59 segment bind at RBD site instead of ACE2 receptor [Figure 5; Table S3b].

## 5. Molecular dynamics simulation

The result of molecular dynamics simulation and normal mode analysis (NMA) of different docked complex of ACE2 and different variants of SARS-CoV 2 is illustrated in Fig 7. The simulation study was conducted to determine the movements of protein molecules. The main-chain deformability graph of the three complexes is shown in S-Fig:1, illustrates the peaks in which represents the regions of the protein with deformability. The locations with hinge regions are high deformability. The B-factor is a measure for flexibility in a protein and quantifies the uncertainty of each. The B-factor values calculated by normal mode analysis are proportional to root mean square shown in Fig 7. B-factor values quantify the uncertainty of each atom. The B-factor graph gives a clear visualization of the relation of the docked complex between the NMA and the PDB sector. The covariance matrix between the pairs of residues is shown in S-Fig:1, indicating their correlations (correlated motion indicated by red color; uncorrelated motion indicating by white color; anti correlated motion indicated by blue color).

We also examined the molecular dynamics simulation of wild59 CUTs and T500S 59 CUTs with Omicron variant is illustrated in Figure 8. The B-factor is a measure for flexibility in a protein and quantifies the uncertainty of each. The B-factor values calculated by normal mode analysis are proportional to root mean square shown in Figure 8. B-factor values quantify the uncertainty of each atom. The B-factor graph gives a clear visualization of the relation of the docked complex between the NMA and the PDB sector. The main-chain deformability graph of the three complexes is shown in S-Fig: 2, illustrates the peaks in which represents the regions of the protein with deformability. The locations with hinge regions are high deformability. The covariance matrix between the pairs of residues is shown in S-Fig: 2, indicating their correlations (correlated motion indicated by red color; uncorrelated motion indicating by white color; anti correlated motion indicated by blue color). So, our all docking complexes are in stable form.

SARS-CoV-2 Omicron RBD shows weaker binding affinity than the currently dominant Delta variant to human ACE2 [32]. Here, we experimentally measure how all amino acid mutations to the RBD affect expression of folded protein and its affinity for ACE2. Most mutations are deleterious for RBD expression and ACE2 binding. But a substantial number of mutations are well tolerated or even enhance ACE2 binding, including at ACE2 interface residues that vary across SARS-related corona viruses. However, we find no evidence that these ACE2-affinity-enhancing mutations have been selected in current SARS-CoV-2 pandemic isolates [33].

Report reveals that infection to Omicron caused an enhancement of Delta virus neutralization, which increased 4.4-fold. This may result in decreased ability of Delta to re-infect those individuals [34]. Omicron mutations enhance infectivity and reduce antibody neutralization of SARS-CoV-2 virus-like particles [35]. Mutations on RBD of SARS-CoV-2 Omicron variant result in stronger binding to human ACE2 receptor [36].

In conclusion, the present 59 amino-acid cut RBD fraction was found to be good blocker of the spike-ACE2 binding. Moreover, introduced mutations especially T500S and T500G were highly potent with very high binding affinity to block the ACE2 and Omicron spike binding. The present investigation may explain Delta variant is significantly stronger than WT and Omicron, while there is no significant difference between Wild type and Omicron but more research is required to explore its less ability to penetrate the lung tissue. This work may not explain the replication/propagation or immuno-invasion ability of omicron. In this case, lung TMPRSS2 may have some role in viral internalization. In regard to the last two years' strategies, global vaccination and natural infection, the disease outcome and severities of different new variants become less predictable. Further studies are required in this regard.

## Declarations

**\*Funding:** No specific funding for this investigation

**\*Conflicts of interest/Competing interests:** none

**\*Availability of data and material:** All data are available upon reasonable requests.

**\*Code availability:** NA

**\*Authors' contributions:** SM- Hypothesis study design, critical analysis and reviewing. DS- Experimentation and first draft preparation.

## References

1. WHO. WHO Coronavirus disease (COVID-19) pandemic. 2021. <https://www.who.int/emergencies/diseases/novel-coronavirus-2019>. Accessed December 7, 2021.
2. Shu Y, McCauley J. GISAID: Global initiative on sharing all influenza data - from vision to reality. *Euro Surveill.* 2017 Mar 30;22(13):30494. doi: 10.2807/1560-7917.ES.2017.22.13.30494. PMID: 28382917; PMCID: PMC5388101.
3. Liu C, Ginn HM, Dejnirattisai W, Supasa P, Wang B, et. al., Reduced neutralization of SARS-CoV-2 B.1.617 by vaccine and convalescent serum. *Cell.* 2021 Aug 5;184(16):4220-4236.e13. doi: 10.1016/j.cell.2021.06.020. Epub 2021 Jun 17. PMID: 34242578; PMCID: PMC8218332.
4. GISAID Tracking of variants. <https://www.gisaid.org/hcov19-variants/> Date: 2021 Date accessed: November 30, 2021

5. Yang T-J, Yu P-Y, Chang Y-C, et al. Impacts on the structure-function relationship of SARS-CoV-2 spike by B.1.1.7 mutations. *bioRxiv*. Published online May 12, 2021. <https://doi.org/10.1101/2021.05.11.443686>.
6. Chen J, Wang R, Gilby NB, Wei GW. Omicron Variant (B.1.1.529): Infectivity, Vaccine Breakthrough, and Antibody Resistance. *J Chem Inf Model*. 2022 Jan 24;62(2):412-422. doi: 10.1021/acs.jcim.1c01451. Epub 2022 Jan 6. PMID: 34989238; PMCID: PMC8751645.
7. Graham F. Daily briefing: Omicron struggles to infect the lungs. *Nature*. 2022 Jan 6. doi: 10.1038/d41586-022-00039-0. Epub ahead of print. PMID: 34997237.
8. Leung K, Shum MH, Leung GM, Lam TT, Wu JT. Early transmissibility assessment of the N501Y mutant strains of SARS-CoV-2 in the United Kingdom, October to November 2020. *Euro Surveill*. 2021 Jan;26(1):2002106. doi: 10.2807/1560-7917.ES.2020.26.1.2002106. Erratum in: *Euro Surveill*. 2021 Jan;26(3): PMID: 33413740; PMCID: PMC7791602.
9. Korber B, Fischer WM, Gnanakaran S, Yoon H, Theiler J, Abfalterer W, Hengartner N, Giorgi EE, Bhattacharya T, Foley B, Hastie KM, Parker MD, Partridge DG, Evans CM, Freeman TM, de Silva TI; Sheffield COVID-19 Genomics Group, McDanal C, Perez LG, Tang H, Moon-Walker A, Whelan SP, LaBranche CC, Saphire EO, Montefiori DC. Tracking Changes in SARS-CoV-2 Spike: Evidence that D614G Increases Infectivity of the COVID-19 Virus. *Cell*. 2020 Aug 20;182(4):812-827.e19. doi: /j.cell.2020.06.043. Epub 2020 Jul 3. PMID: 32697968; PMCID: PMC7332439.
10. Plante JA, Liu Y, Liu J, Xia H, Johnson BA, Lokugamage KG, Zhang X, Muruato AE, Zou J, Fontes-Garfias CR, Mirchandani D, Scharton D, Bilello JP, Ku Z, An Z, Kalveram B, Freiberg AN, Menachery VD, Xie X, Plante KS, Weaver SC, Shi PY. Spike mutation D614G alters SARS-CoV-2 fitness. *Nature*. 2021 Apr;592(7852):116-121. doi: 10.1038/s41586-020-2895-3. Epub 2020 Oct 26. Erratum in: *Nature*. 2021 Jul;595(7865):E1. PMID: 33106671; PMCID: PMC8158177.
11. Volz E, Hill V, McCrone JT, Price A, Jorgensen D, O'Toole Á, Southgate J, Johnson R, Jackson B, Nascimento FF, Rey SM, Nicholls SM, Colquhoun RM, da Silva Filipe A, Shepherd J, Pascall DJ, Shah R, Jesudason N, Li K, Jarrett R, Pacchiarini N, Bull M, Geidelberg L, Siveroni I; COG-UK Consortium, Goodfellow I, Loman NJ, Pybus OG, Robertson DL, Thomson EC, Rambaut A, Connor TR. Evaluating the Effects of SARS-CoV-2 Spike Mutation D614G on Transmissibility and Pathogenicity. *Cell*. 2021 Jan 7;184(1):64-75.e11. doi: 10.1016/j.cell.2020.11.020. Epub 2020 Nov 19. PMID: 33275900; PMCID: PMC7674007.
12. Planas D, Saunders N, Maes P, Guivel-Benhassine F, Planchais C, Buchrieser J, Bolland WH, Porrot F, Staropoli I, Lemoine F, Péré H, Veyer D, Puech J, Rodary J, Baele G, Dellicour S, Raymenants J, Gorissen S, Geenen C, Vanmechelen B, Wawina-Bokalanga T, Martí-Carreras J, Cuypers L, Sève A, Hocqueloux L, Prazuck T, Rey F, Simon-Loriere E, Bruel T, Mouquet H, André E, Schwartz O. Considerable escape of SARS-CoV-2 Omicron to antibody neutralization. *Nature*. 2021 Dec 23. doi: 10.1038/s41586-021-04389-z. Epub ahead of print. PMID: 35016199.
13. Liu L, Iketani S, Guo Y, Chan JF, Wang M, Liu L, Luo Y, Chu H, Huang Y, Nair MS, Yu J, Chik KK, Yuen TT, Yoon C, To KK, Chen H, Yin MT, Sobieszczyk ME, Huang Y, Wang HH, Sheng Z, Yuen KY, Ho DD.

- Striking Antibody Evasion Manifested by the Omicron Variant of SARS-CoV-2. *Nature*. 2021 Dec 23. doi: 10.1038/s41586-021-04388-0. Epub ahead of print. PMID: 35016198.
14. Nishiura H, Ito K, Anzai A, Kobayashi T, Piantham C, Rodríguez-Morales AJ. Relative Reproduction Number of SARS-CoV-2 Omicron (B.1.1.529) Compared with Delta Variant in South Africa. *J Clin Med*. 2021 Dec 23;11(1):30. doi: 10.3390/jcm11010030. PMID: 35011781; PMCID: PMC8745053.
  15. Yang G, Tan Z, Zhou L, Yang M, Peng L, Liu J, Cai J, Yang R, Han J, Huang Y, He S. Effects of Angiotensin II Receptor Blockers and ACE (Angiotensin-Converting Enzyme) Inhibitors on Virus Infection, Inflammatory Status, and Clinical Outcomes in Patients With COVID-19 and Hypertension: A Single-Center Retrospective Study. *Hypertension*. 2020 Jul;76(1):51-58. doi: 10.1161/HYPERTENSIONAHA.120.15143. Epub 2020 Apr 29. PMID: 32348166.
  16. Science Brief: Omicron (B.1.1.529) variant. CDC. Accessed December 4, 2021. <https://www.cdc.gov/coronavirus/2019-ncov/science/science-briefs/scientific-brief-omicron-variant.html>.
  17. Banerjee A, Kanwar M, Santra D, Maiti S. Conserved in 186 countries the RBD fraction of SARS CoV-2 S-protein with in –silico T500S mutation strongly blocks ACE2 rejecting the viral spike: A Molecular-docking analysis. *bioRxiv* 2021.04.25.441361; doi: <https://doi.org/10.1101/2021.04.25.441361>.
  18. W.L. DeLano Pymol: An open-source molecular graphics tool *CCP4 Newsletter On Protein Crystallography*, 40 (2002), pp. 82-92.
  19. Lovell SC, Davis IW, Arendall WB 3rd, de Bakker PI, Word JM, Prisant MG, Richardson JS, Richardson DC. Structure validation by Calpha geometry: phi,psi and Cbeta deviation. *Proteins*. 2003 Feb 15;50(3):437-50. doi: 10.1002/prot.10286. PMID: 12557186.
  20. Honorato RV, Koukos PI, Jiménez-García B, Tsaregorodtsev A, Verlatto M, Giachetti A, Rosato A, Bonvin AMJJ. Structural Biology in the Clouds: The WeNMR-EOSC Ecosystem. *Front Mol Biosci*. 2021 Jul 28;8:729513. doi: 10.3389/fmolb.2021.729513. PMID: 34395534; PMCID: PMC8356364.
  21. Vangone A, Bonvin AM. Contacts-based prediction of binding affinity in protein-protein complexes. *Elife*. 2015 Jul 20;4:e07454. doi: 10.7554/eLife.07454. PMID: 26193119; PMCID: PMC4523921.
  22. López-Blanco JR, Aliaga JI, Quintana-Ortí ES, Chacón P. iMODS: internal coordinates normal mode analysis server. *Nucleic Acids Res*. 2014 Jul;42(Web Server issue):W271-6. doi: 10.1093/nar/gku339. Epub 2014 Apr 25. PMID: 24771341; PMCID: PMC4086069.
  23. Kabsch W. A solution for the best rotation to relate two sets of vectors. *Acta Crystallogr. A*. 1976;32:922–923.
  24. Damm KL, Carlson HA. Gaussian-weighted RMSD superposition of proteins: a structural comparison for flexible proteins and predicted protein structures. *Biophys J*. 2006 Jun 15;90(12):4558-73. doi: 10.1529/biophysj.105.066654. Epub 2006 Mar 24. PMID: 16565070; PMCID: PMC1471868.
  25. Meo SA, Meo AS, Al-Jassir FF, Klonoff DC. Omicron SARS-CoV-2 new variant: global prevalence and biological and clinical characteristics. *Eur Rev Med Pharmacol Sci*. 2021 Dec;25(24):8012-8018. doi: 10.26355/eurrev\_202112\_27652. PMID: 34982465.

26. Khan K, Karim F, Cele S, San JE, Lustig G, Tegally H, Bernstein M, Ganga Y, Jule Z, Reedoy K, Ngcobo N, Mazibuko M, Mthabela N, Mhlane Z, Mbatha N, Giandhari J, Ramphal Y, Naidoo T, Manickchand N, Magula N, Karim SSA, Gray G, Hanekom W, von Gottberg A; COMMIT-KZN Team, Gosnell BI, Lessells RJ, Moore PL, de Oliveira T, Moosa MS, Sigal A. Omicron infection enhances neutralizing immunity against the Deltavariant. medRxiv [Preprint]. 2021 Dec 27:2021.12.27.21268439. doi: 10.1101/2021.12.27.21268439. Update in: Nature. 2021 Dec 23; PMID: 34981076; PMCID: PMC8722619.
27. Maiti S, Banerjee A, Kanwar M. In silico Nigellidine (*N. sativa*) bind to viral spike/active-sites of ACE1/2, AT1/2 to prevent COVID-19 induced vaso-tumult/vascular-damage/comorbidity. *Vascul Pharmacol.* 2021 Jun;138:106856. doi: 10.1016/j.vph.2021.106856. Epub 2021 Mar 18. PMID: 33746069; PMCID: PMC7970800.
28. D. Halliday, R. Resnick, J. Walker Electric potential Fundamentals of Physics (5th ed.), John Wiley & Sons (1997) ISBN 0-471-10559-7.
29. E.M. Purcell Electricity and Magnetism Cambridge University Press (2013), pp. 16-18 ISBN 978-1107014022
30. Wu L, Zhou L, Mo M, Liu T, Wu C, Gong C, Lu K, Gong L, Zhu W, Xu Z. SARS-CoV-2 Omicron RBD shows weaker binding affinity than the currently dominant Deltavariant to human ACE2. *Signal Transduct Target Ther.* 2022 Jan 5;7(1):8. doi: 10.1038/s41392-021-00863-2. PMID: 34987150; PMCID: PMC8727475.
31. Starr TN, et al. Deep mutational scanning of SARS-CoV-2 receptor binding domain reveals constraints on folding and ACE2 binding. *Cell.* 2020;182:1295–1310.e20. doi: 10.1016/j.cell.2020.08.012.
32. Wu L, Zhou L, Mo M, Liu T, Wu C, Gong C, Lu K, Gong L, Zhu W, Xu Z. SARS-CoV-2 Omicron RBD shows weaker binding affinity than the currently dominant Deltavariant to human ACE2. *Signal Transduct Target Ther.* 2022 Jan 5;7(1):8. doi: 10.1038/s41392-021-00863-2. PMID: 34987150; PMCID: PMC8727475.
33. Starr TN, Greaney AJ, Hilton SK, Ellis D, Crawford KHD, Dingens AS, Navarro MJ, Bowen JE, Tortorici MA, Walls AC, King NP, Velesler D, Bloom JD. Deep Mutational Scanning of SARS-CoV-2 Receptor Binding Domain Reveals Constraints on Folding and ACE2 Binding. *Cell.* 2020 Sep 3;182(5):1295-1310.e20. doi: 10.1016/j.cell.2020.08.012. Epub 2020 Aug 11. PMID: 32841599; PMCID: PMC7418704.
34. Khan K, Karim F, Cele S, San JE, Lustig G, Tegally H, Bernstein M, Ganga Y, Jule Z, Reedoy K, Ngcobo N, Mazibuko M, Mthabela N, Mhlane Z, Mbatha N, Giandhari J, Ramphal Y, Naidoo T, Manickchand N, Magula N, Karim SSA, Gray G, Hanekom W, von Gottberg A; COMMIT-KZN Team, Gosnell BI, Lessells RJ, Moore PL, de Oliveira T, Moosa MS, Sigal A. Omicron infection enhances neutralizing immunity against the Deltavariant. medRxiv [Preprint]. 2021 Dec 27:2021.12.27.21268439. doi: 10.1101/2021.12.27.21268439. Update in: Nature. 2021 Dec 23; PMID: 34981076; PMCID: PMC8722619.

35. Syed AM, Ciling A, Khalid MM, Sreekumar B, Chen PY, Kumar GR, Silva I, Milbes B, Kojima N, Hess V, Shacreaw M, Lopez L, Brobeck M, Turner F, Spraggon L, Taha TY, Tabata T, Chen IP, Ott M, Doudna JA. Omicron mutations enhance infectivity and reduce antibody neutralization of SARS-CoV-2 virus-like particles. medRxiv [Preprint]. 2022 Jan 2:2021.12.20.21268048. doi: 10.1101/2021.12.20.21268048. PMID: 34981067; PMCID: PMC8722610.
36. Lupala CS, Ye Y, Chen H, Su XD, Liu H. Mutations on RBD of SARS-CoV-2 Omicron variant result in stronger binding to human ACE2 receptor. Biochem Biophys Res Commun. 2022 Jan 29;590:34-41. doi: 10.1016/j.bbrc.2021.12.079. Epub 2021 Dec 24. PMID: 34968782; PMCID: PMC8702632.

## Figures

### Figure 1

Individual molecular docking of ACE2 receptor and spike glycoproteins- A) ACE2 with Wild SARS-COV-2 binding; B) ACE2 with DELTAVariant; C) ACE2 with Omicron variant. The binding between ACE2 and three spike proteins shown in various position of amino acids.



## Figure 2

The superposition of the docked complexes of SARS-COV2 and Omicron spike proteins binding with Human ACE2 receptor was presented- a)The enlarged panel on the right side shows the interacting amino acid residues in colored sticks in which SARS-CoV-2 is red, b) the left side shows the Omicron mutant variant in pink. In both enlarged colored sticks ACE2 receptor indicated with blue. Omicron variant interact with ACE2 receptor in 3 different amino acid positions which was indicated in table form.

## Figure 3

The superposition of the docked complexes of Delta and Omicron spike proteins binding with Human ACE2 receptor was presented. The enlarged panel on the left side shows the interacting amino acid residues in colored sticks in which Delta is in green color and ACE2 receptor indicated with blue. On the other hand, Omicron variant does not interact with ACE2 receptor. Delta variant interact with ACE2 receptor in 3 different amino acid positions which was indicated in table form.





## Figure 4

The superposition of the docked complexes of SARS-CoV-2, Delta and Omicron spike proteins binding with Human ACE2 receptor was presented-a) The enlarged panel on the right side shows the interacting amino acid residues in colored sticks in which Delta is in green color and ACE2 receptor indicated with blue, b) the left side shows the interacting amino acid residues in colored sticks in which Omicron variant is in pink and ACE2 receptor is in blue. Wild SARS-CoV-2 totally blocked by other two types of variant and do not interact with ACE2 at binding site. Delta variant interact with ACE2 receptor in 4 different amino acid positions and Omicron variant interact with ACE2 receptor in 2 different amino acid positions which was indicated in table form. So, the binding comparison between 3 spike glycoproteins with ACE2 receptor, Delta variant has highest binding positions with receptor than other 2 types spike glycoproteins.

## Figure 5

The Molecular docking of ACE2, Omicron variant and Wild 59 cut was presented -A and B) the enlarged panel on the left side shows the interacting amino acid residues in colored sticks in which ACE2 is in blue and Omicron variant is in orange; C,D,E,F) the enlarged panel on right side shows the interacting amino acid residues in which Omicron is in orange and Wild 59 cut is in red.



## Figure 6

The Molecular docking of ACE2, Omicron variant and Mutant 59 cut- A and B) the enlarged panel on the left side shows the interacting amino acid residues in colored sticks in which ACE2 is in blue and Omicron variant is in orange; C,D,E) the enlarged panel on right side shows the interacting amino acid residues in which Omicron is in orange and mutant 59 cut is in green.

**Figure 7**

The results of molecular dynamics simulation of different variant of SARS-CoV 2 and ACE2 docked complex. (A,B) RMSD plot and Bfactor graph of wild type SARS-CoV2 and ACE2; (C,D) RMSD plot and Bfactor graph of Delta and ACE2 , (E, F) RMSD plot and Bfactor graph of Omicron and ACE2.

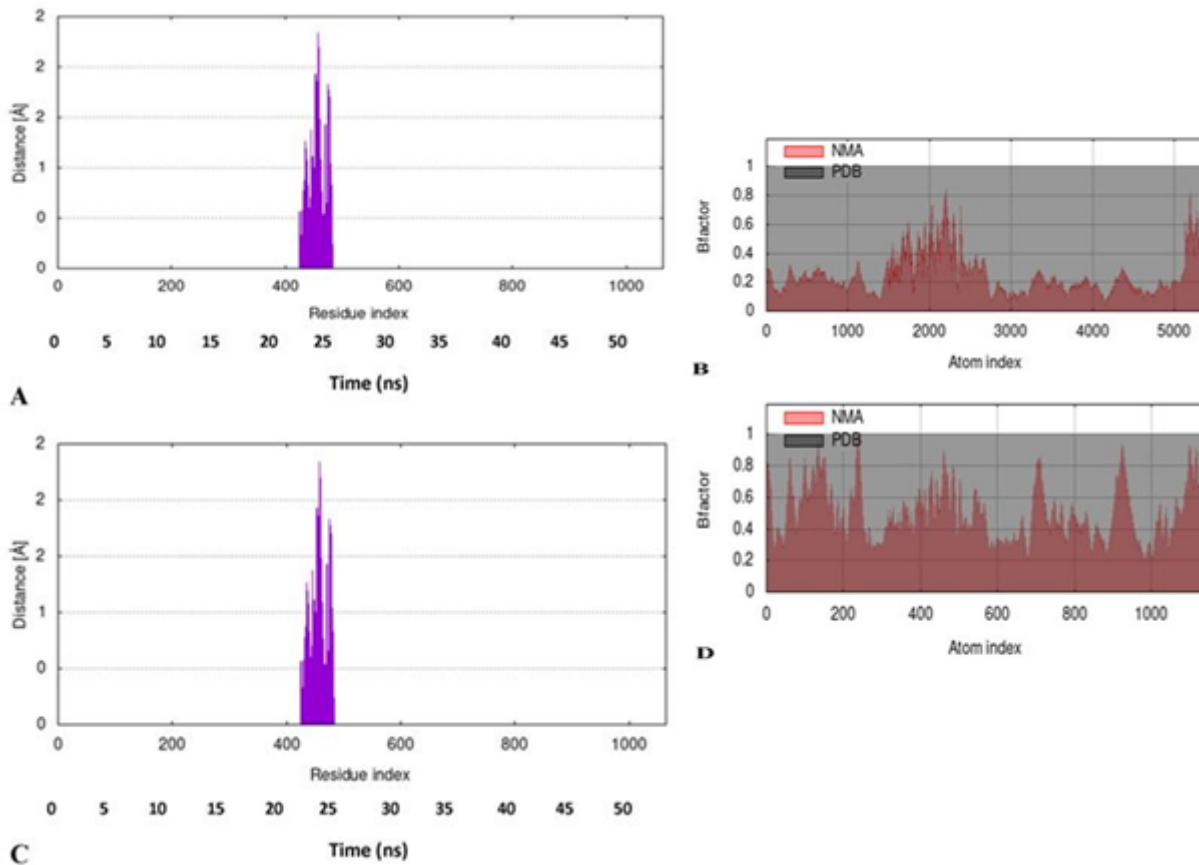


**Figure 8**

The results of molecular dynamics simulation of two CUTs 59 sequence with Omicron variants docked complex. (A,B) RMSD plot and Bfactor graph of wild59 CUTs and Omicron; (C,D) RMSD plot and Bfactor graph of T500S 59 CUTs sequence and Omicron.

## Supplementary Files

This is a list of supplementary files associated with this preprint. Click to download.

- [Supplementaryfile1.docx](#)